Kinetics of equilibrium passive sampling of organic chemicals with polymers in diverse mammalian tissues

Andreas Baumer,[a] Sandra Jäsch,[b] Nadin Ulrich,[b] Ingo Bechmann,[c] Julia Landmann,[c] Beate I. Escher [a,d] *

[a]*Department Cell Toxicology, Helmholtz Centre for Environmental Research– UFZ, 04318 Leipzig, Germany*

[b]*Department Analytical Environmental Chemistry, Helmholtz Centre for Environmental Research– UFZ, 04318 Leipzig, Germany*

[c]*Institute of Anatomy, University of Leipzig, 04103 Leipzig, Germany*

[d]*Environmental Toxicology, Centre for Applied Geosciences, Eberhard Karls University Tübingen, 72076 Tübingen, Germany*

*Corresponding Author

Beate I. Escher, UFZ − Helmholtz Centre for Environmental Research, Permoserstr 15, 04318 Leipzig, Germany; Tel. +49 341 235 1244. Fax+49 341 235 1244. Email: beate.escher@ufz.de.

ABSTRACT

Equilibrium passive sampling employing polydimethylsiloxane (PDMS) as sampling phase can be used for the extraction of complex mixtures of organic chemicals from lipid-rich biota. We extended the method to lean tissues and more hydrophilic chemicals by implementing a mass-balance model for partitioning between lipids, proteins and water in the tissues and by accelerating uptake kinetics with a custom-built stirrer that effectively decreased time to equilibrium to less than 8 days even for homogenized liver tissue with only 4% lipid content. The partition constants $\log K_{\mathrm{lipid/PDMS}}$ between tissues and PDMS were derived from measured concentration in PDMS and the mass-balance model and were very similar for 40 neutral chemicals with octanol-water partition constants $1.4 < \log K_{\mathrm{ow}} < 8.7$, that is, $\log K_{\mathrm{lipid/PDMS}}$ of 1.26 (95% CI 1.13 – 1.39) for adipose tissue, 1.16 (1.00 – 1.33) for liver and 0.58 (0.42 – 0.73) for brain. This conversion factor can be applied to interpret chemical analysis and *in vitro* bioassays after additionally accounting for small fractions of coextracted lipids of < 0.7% of PDMS weight. PDMS is more widely applicable for passive sampling of mammalian tissues than previously thought, both, in terms of diversity of chemicals and range of lipid content of tissues and, therefore, an ideal method for human biomonitoring to be combined with *in vitro* bioassays.

SYNOPSIS

Complex mixtures of hydrophilic and hydrophobic chemicals can be extracted with silicone from mammalian tissues no matter what the lipid content is.

KEYWORDS

Mixture, passive sampling, extraction, biomonitoring, *in vitro* bioassays

TOC ART

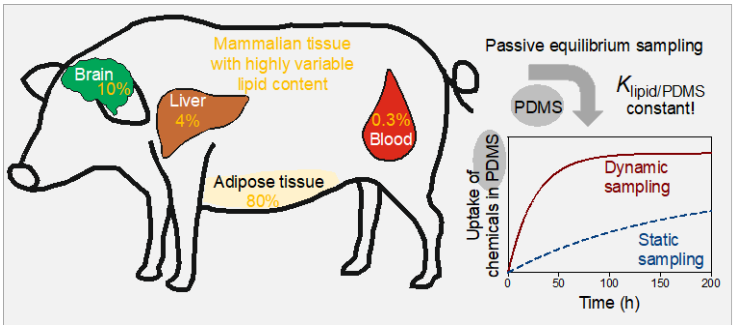

INTRODUCTION

Although the production of persistent organic pollutants (POPs) like polychlorinated biphenyls (PCBs), polybrominated diphenyl ethers (PBDEs) and organochlorine pesticides (OCPs) was banned and their usage was restricted by the Stockholm Convention,[1] these harmful chemicals can still be detected ubiquitously and pose a risk.[2] Due to their hydrophobicity and stability against degradation processes, POPs tend to bioaccumulate in lipid-rich tissues across food webs and can be measured in living organisms such as benthic invertebrates[3], fish[4], marine mammals[5-7] and humans.[8-10] Quantification of POPs in tissues typically involves exhaustive solvent extraction methods followed by silica gel and sulphuric acid clean-up in order to remove coextracted matrix components before instrumental analysis.[5, 8, 10]

More polar chemicals may also be present in mammalian tissue and blood and are of interest for biomonitoring.[11, 12] Polar chemicals are poorly recovered by extraction with non-polar solvents and degraded by destructive clean-up procedures. Alternatives are polar solvent extraction (e.g., with acetonitrile) followed by non-destructive clean-ups like dispersive solid phase extraction (dSPE),[13] gel permeation chromatography (GPC) or low temperature precipitation (freeze-out) for extract purification.[7, 14] Such methods have been applied to blood,[15] breast milk,[14] fish[16] and liver tissue[17] but are restricted to tissues of lower lipid content and recovery is decreasing with increasing hydrophobicity.[18, 19]

Passive equilibrium sampling employing polydimethylsiloxane (PDMS) is well-established for the extraction of complex chemical mixtures from biological fluids,[20, 21] lipid-rich tissues like blubber[22, 23] and fatty fish.[24] Equilibrium is attained rapidly within few hours due to fast intra-tissue diffusion in lipid-rich biota tissues.[22, 25, 26] Even in liquid suspensions like blood, colloidal lipids and proteins serve as transport agents for the chemicals, thus, accelerating the time to reach equilibrium.[21] In contrast, passive sampling in lean biota tissues (< 10% lipid content) is challenging, because local depletion near the sampler surface results in slow uptake rates of the chemicals into the PDMS. As a consequence, equilibrium is not attained within a week.[24] This issue can be overcome by multiple manual relocations of the silicone to assure that fresh tissue is constantly in contact with the sampler.[27, 28] But this bears the risk of sample contamination and involves time-intense laboratory logistics. Rolling thin PDMS sheets in jars together with tissue cubes or homogenates is an alternative sampling method for lean fish tissues.[27, 29]

PDMS extracts can be subjected without extensive clean-up to instrumental analysis[30] and bioanalytical screening[21, 23, 26], because only small amounts of unwanted matrix is coextracted. Especially in toxicological screening studies using cell based *in-vitro* bioassays, conserving the original mixture composition is important, because the losses of analytes during clean-up stages cannot be corrected with recovery standards and extensive extraction and clean-up procedures might cause contamination and blank effects.[2, 31] The aim of the study was to develop an extraction method employing equilibrium passive

sampling with PDMS to tissues of variable lipid content and extending the range from hydrophobic to hydrophilic neutral chemicals. Quantification of less persistent and more hydrophilic and polar alongside persistent and hydrophobic chemicals in lipids and tissues is technically challenging and elaborate clean-up steps were circumvented by the passive sampling with PDMS combined with a mass balance model that was validated by comparison of the resulting partition constants with literature data.

THEORY

Passive equilibrium sample has been mainly applied for sampling hydrophobic organic chemicals in tissues high in lipid content such as blubber or adipose tissue, where all concentrations could be normalized to the lipid content. To extent the approach to tissue of any composition, including water- and protein-rich blood, lean muscle tissue and organs such as liver and brain, partitioning of chemicals between lipid, protein and water in tissue (Figure 1A) has to be included in the model, with tissue concentrations (C_{tissue}) of chemicals defined by eq.1, where C are the concentrations in lipids (C_{lipid}), proteins ($C_{protein}$) and water (C_{water}), and mf are the mass fractions of the lipids ($mf_{lipid} = m_{lipid}\ m_{tissue}^{-1}$), proteins ($mf_{protein} = m_{protein}\ m_{tissue}^{-1}$), water ($mf_{water} = m_{water}\ m_{tissue}^{-1}$) and the residual weight ($mf_{residual}$).

$$C_{tissue} = mf_{lipid}\ C_{lipid} + mf_{protein}\ C_{protein} + mf_{water}\ C_{water} + mf_{residual} \quad (1)$$

C_{tissue} can be based on lipid concentrations (eq.2) if the partition constants between lipid and protein, $K_{lipid/protein}$, and lipid and water, $K_{lipid/water}$ are known. The $mf_{residual}$ is assumed to be non-binding and was therefore neglected in eq. 2.

$$C_{tissue} = \left(mf_{lipid} + \frac{mf_{protein}}{K_{lipid/protein}} + \frac{mf_{water}}{K_{lipid/water}}\right) C_{lipid} \quad (2)$$

In Figure 1B, the role is explored that proteins and water play for partitioning. If a tissue is lipid-rich, e.g., composed of 80% lipids, 10% proteins and 10% water, partitioning to proteins and water does not play a role, even for the most hydrophilic chemicals because $mf_{protein}/K_{lipid/protein}$ and $mf_{water}/K_{lipid/water}$ are negligible against mf_{lipid} (Figure 1B). If the tissue is lean, e.g., composed of 10% lipids, 30% proteins and 60% water, then binding to lipids still is expected to dominate with exception of chemicals with $\log K_{lipid/water} < 2$, where a substantial fraction of chemicals would be expected to stay in water, i.e., $mf_{water}/K_{lipid/water} > mf_{lipid}/K_{lipid/lipid}$ (= mf_{lipid}) (Figure 1B). For blood, composed of approximately 0.5% lipids, 20% proteins and 80% water, both lipids and proteins play a role with protein being dominant, and the aqueous concentration cannot be neglected for hydrophilic chemicals with $\log K_{lipid/water} < 3$ (Figure 1B).

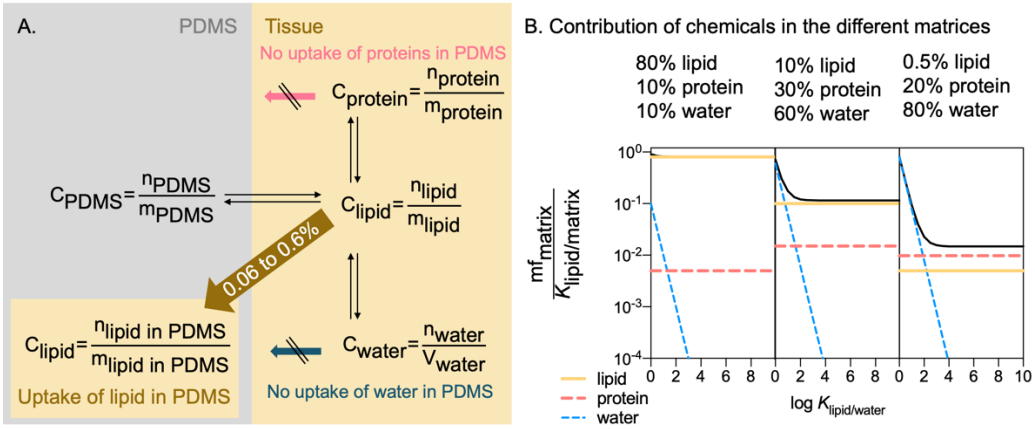

Figure 1 A. Partitioning and binding processes relevant in passive equilibrium sampling of neutral organic chemicals in tissue. **B.** Contribution of chemicals in the different phases, expressed as $mf_{matrix}/K_{lipid/matrix}$, where matrix is lipid (yellow), protein (red) or water (blue), and the black line is the sum of all fractions. For these simulations it was assumed that $K_{lipid/protein}$ is approximately 20.[32]

During the extraction, a small fraction of lipid might be taken up into PDMS (Figure 1A), typically much less than 1% of the PDMS weight. A mass-balance model (MBM) describes all partitioning processes and uptake of lipids into PDMS. If it is assumed that the concentration of chemicals in lipid inside PDMS is the same as in the lipid of the tissue, the concentration in lipids in equilibrium with PDMS can be calculated by eq.3, where n_{tot} is the total concentration of the chemical in the system, $n_{extract}$ is the concentration in the extract of PDMS.

$$C_{lipid}=\frac{n_{tot}-n_{extract}}{m_{lipid}-\Delta m_{PDMS}+\frac{m_{protein}}{K_{lipid/protein}}+\frac{m_{water}}{K_{lipid/water}}} \quad (3)$$

The true concentration of a chemical in PDMS can accordingly be calculated from the amount in the extract after subtracting the contribution of the chemical in the lipid taken up into PDMS (Δm_{PDMS}) using eq.4, where m_{PDMS} is the mass of PDMS prior to passive sampling.

$$C_{PDMS}=\frac{n_{PDMS}}{m_{PDMS}}=\frac{n_{extract}-C_{lipid}\times\Delta m_{PDMS}}{m_{PDMS}} \quad (4)$$

The partition constant between lipids and PDMS, $K_{lipid/PDMS}$, is then defined by eq.5.

$$K_{lipid/PDMS}=\frac{C_{lipid}}{C_{PDMS}} \quad (5)$$

For tissues with a substantial lipid content (adipose tissue, liver, brain), the $K_{lipid/PDMS}$ was converted to $K_{tissue/PDMS}$ by inserting eq.2 in eq.5, which yields eq.6.

$$K_{tissue/PDMS}=\left(mf_{lipid}+\frac{mf_{protein}}{K_{lipid/protein}}+\frac{mf_{water}}{K_{lipid/water}}\right)K_{lipid/PDMS} \quad (6)$$

For blood with its low lipid content, where passive sampling would be used either in a depletive mode or by measuring $K_{\text{tissue/PDMS}}$, $K_{\text{tissue/PDMS}}$ can be converted to $K_{\text{lipid/PDMS}}$ with eq.7 for comparison of concentrations in blood and other tissues.

$$K_{\text{lipid/PDMS}} = \frac{K_{\text{tissue/PDMS}}}{\left(\text{mf}_{\text{lipid}} + \frac{\text{mf}_{\text{protein}}}{K_{\text{lipid/protein}}} + \frac{\text{mf}_{\text{water}}}{K_{\text{lipid/water}}}\right)} \quad (7)$$

As discussed above, the term $\frac{\text{mf}_{\text{water}}}{K_{\text{lipid/water}}}$ is negligible for chemicals of medium and high hydrophobicity, so the $K_{\text{lipid/protein}}$ would be the main input parameter apart from the tissue properties mf_{lipid} and $\text{mf}_{\text{protein}}$, which can be measured as described below or taken from literature.[33]

When applying simple partitioning models to estimate partitioning between organs and tissues, previous work has differentiated between neutral and phospholipids as well as between storage and membrane lipids.[34] For neutral chemicals, there is little difference between $K_{\text{storage lipid/water}}$ and $K_{\text{membrane lipid/water}}$,[35] and both can be satisfactorily approximated by the octanol-water partition constant $\log K_{\text{ow}}$,[35, 36] while the difference is very important for ionizable organic chemicals.[37]

Binding to proteins is very much dependent on the protein type and especially anionic organic chemicals show large differences between structural and serum proteins as well as strong saturation effects and multiphasic binding.[38, 39] For neutral organic chemicals, one can describe protein binding as a partitioning process, and the binding to chicken muscle protein was approximately 7 times lower than to serum albumin.[40] Only in serum, albumin is the dominant protein, in most other tissues and whole blood (as applied in the present study), there are at least ten times more structural proteins than albumins.[40] deBruyn et al.[32] established a $\log K_{\text{ow}}$–$\log K_{\text{protein/water}}$ relationship over a wide range of hydrophobicity which was also confirmed by Endo's study[40] using muscle protein, resulting in an approximate $K_{\text{lipid/protein}}$ of 20, which was used in the present study. These previous studies used volume-based partition constants, while here the partitioning model is based on masses of the partitioning matrices. With a density of approximately 1 kg L^{-1} for lipids and of 1.4 kg L^{-1} for proteins,[40] the impact of this conversion is small (0.15 log-units for proteins, no change for lipids) and within the parameter uncertainty and therefore we did not implement any further corrections. The $K_{\text{lipid/protein}}$ of 20 implies that the binding to proteins only play a role if the protein content is at least as high as the lipid content, which is expected to be the case for liver and blood.[33]

MATERIAL AND METHODS

Chemicals and materials. Chemicals and internal standard and their suppliers can be found in the Supporting Information (Tables S1-S3). PDMS sheets (SSP-M823, Special Silicone Products, Ballston, USA) with thicknesses of 1, 0.63, 0.33 and 0.25 mm and a density of 1.17 g cm^{-3} were purchased from Shielding Solutions (Great Notley, Great Britain).

The physicochemical properties, including logK_{ow}, the PDMS-water partition constant log$K_{PDMS/water}$, the liposome-water partition constant log$K_{liposome/water}$ as a proxy of log$K_{membrane\ lipid/water}$, log$K_{storage\ lipid/water}$, the partition constants between bovine serum albumin (BSA) or chicken muscle protein and water (log$K_{BSA/water}$ and log$K_{muscle\ protein/water}$, respectively) as a proxy of log$K_{protein/water}$ are listed in Table S1. They were retrieved from literature and missing values were filled by Linear Solvation Energy Relationship (LSER) [41] or, if no descriptors for LSER were available, by Quantitative Structure Activity relationships (QSAR) using the logK_{ow} as descriptor [40, 42, 43] The partition constants in the present study are expressed as mass ratio, and most of the literature *K* were given in these units, with some exceptions and some studies where the units were not defined. As is the case for proteins and lipids discussed above, the error in case of log$K_{PDMS/water}$ would be 0.07, which is negligible as compared to the uncertainty of the actual parameters, hence no density corrections were performed.

Tissue and blood samples. Pork tissues (liver, brain, and adipose tissue) were bought in a local butchery. Whole blood from pig was obtained from Fiebig-Nährstofftechnik (Idstein-Niederauroff, Germany) containing 1.5 mg ethylenediaminetetraacetic acid dipotassium salt per mL whole blood preventing coagulation. All tissues were homogenized using a blender (B-400, BÜCHI Labortechnik AG, Switzerland). Homogenized tissues as well as whole blood samples were stored at -20 °C until analysis.

Determination of lipid content was carried out gravimetrically after solvent extraction employing a mixture of cyclohexane, 2-propanol and water according to Smedes[44] with modifications described in Text S1. For the determination of total protein content, a Thermo Scientific™ Pierce™ BCA Protein Assay Kit (Thermo Scientific, USA) was used and with modifications described in Text S2. The water content of the tissues and blood was measured by the weight loss after drying 0.5 to 1 g of tissue homogenate or whole blood at 105 °C for 24 h.

Spiking of tissue with a defined mixture of chemicals. The 40 chemicals listed in Table S1 were spiked to the three tissues and blood dissolved in ethyl acetate as described in Text S3. The final concentrations of each chemical in adipose tissue were in the range of 300 and 8000 ng $g_{adipose\ tissue}^{-1}$. Blood concentrations ranged between 15 and 36 ng mL_{blood}^{-1}. Concentrations in liver tissue were in the range of 100 and 500 ng $g_{liver\ tissue}^{-1}$ and in brain 20 and 600 ng $g_{brain\ tissue}^{-1}$.

Passive sampling of tissues and blood. PDMS to tissue ratios used in the passive sampling experiments were calculated based on the negligible depletion criterion[24] using an initial average $K_{lipid/PDMS}$ [L_{PDMS} L_{lipid}^{-1}] value of 30 estimated from previous work[23] (Text S4). 0.4 g adipose tissue were sampled with 125 mg PDMS, 3 g liver and brain tissue with 250 mg PDMS. For blood, a lower blood to PDMS volume ratio of

2.2 mL blood with 400 mg PDMS was used to ensure a nearly exhaustive extraction (60 – 80% mass transfer) as described for turtle blood by Jin et al.[21]

Solvent-cleaned (Text S5) PDMS disks (12 mm diameter, 28 to 127 mg) were statically exposed to 385 – 420 mg adipose tissue by sandwiching the disks between two tissue layers as illustrated in Figure S1 inside the cavities of stainless-steel blocks. A metal pin was used for sealing and to put pressure for enhancing the contact between tissue and PDMS (Figure S1).

All other tissues were extracted with PDMS strips in what was termed "dynamic passive sampling", i.e., aided by moving the PDMS through the tissue to avoid local depletion. In case of blood, the PDMS (60 × 10 × 0.6 mm) was tightly fixed in a 4 mL vial that was sealed with a cap containing a PTFE septum after the blood sample was added. The vial was placed on a roller mixer (Ratek, Fröbel Labortechnik, Germany) at a speed of 10 rpm for extraction. With every rotation of the vial, the wings formed by the PDMS assured that the blood was thoroughly mixed (Figure S2).

Dynamic passive sampling experiments with 3.2 – 3.8 g homogenized liver and 2.6 – 3.3 g brain tissue were performed in 4 mL vials using a custom-built mixing instrument. The PDMS strips (45 to 55 × 5 × 1 mm, 240 – 366 mg (Tables S9 and S11) were fixed on a stainless-steel rod, which was connected to an electric motor (Figure S3). With a speed of 120 rpm, the PDMS wings ensured an appropriate mixing of the tissue that was necessary to avoid local depletion issues occurring in lean tissues. No water was added, the stirrer had enough power to mix the homogenized tissue.

All dynamic passive sampling experiments were carried out at 4 – 8 °C to slow down tissue decay during sampling time span of 7 days. At defined time points up to 200 h, the PDMS sampler were retrieved from the tissue and cleaned with lint-free paper wipes and MilliQ water. After the cleaning, PDMS weight gain by the co-extracted matrix components was recorded. The internal standards (Table S2) were spiked on the surface of the PDMS. PDMS was extracted twice with 1 mL ethyl acetate per 0.1 g PDMS for 2 h on a roller mixer, which is a 20 fold excess of the amount of ethyl acetate required for complete extraction (for partition constants between PDMS and ethyl acetate see ref.[45]). The lipid taken up into the PDMS could also be completely extracted with this method as a control experiment demonstrated where a 100 mg PDMS disk that was loaded with 1 mg triolein and the 1 mg was confirmed gravimetrically in the evaporated ethyl acetate extract.

The volume of the combined solvent extracts was reduced under a gentle stream of nitrogen using an XcelVap automated evaporation and concentration system from Horizon Technologies (Axel Semrau, Sprockhövel, Germany). The extract was transferred to a 1.5 mL vial, the solvent was blown down to dryness and reconstituted in 50 µL ethyl acetate. The vials were stored in a freezer at -20 °C until analysis.

Instrumental analysis. The chemicals in the solvent extracts were quantified with a previously described GC-MS/MS method by Baumer et al.[30] employing direct sample introduction (DSI) approach with minor

modifications (Text S6, Tables S4 and S5) using an Agilent 7890 GC system with a 7010 Triple Quadrupole MS (Agilent Technologies, USA). For injection, a Thermal Desorption Unit (TDU 2) combined with a Cold Injection System (CIS 4, GERSTEL GmbH, Mülheim a. d. Ruhr, Germany) was applied.

Data evaluation. Eqs. 3 and 4 hold strictly only true for equilibrium conditions, which only applied to the extraction of adipose tissue. For blood, liver and brain, equilibrium $K_{PDMS/lipid}$ was extrapolated from uptake kinetics curves.

For blood, we plotted the ratio of $n_{extract}/n_{tot}$ against the time t and derived the uptake rate constant k_{uptake} with eq. 8. If the extraction is fully depletive, $n_{extract}/n_{tot}$ reaches 1.

$$\frac{n_{extract}}{n_{tot}}(t)=\frac{n_{extract}}{n_{tot}}(max)\times\left(1-e^{-k_{uptake}\times t}\right) \quad (8)$$

For liver and brain tissue, the ratios of $C_{PDMS}(t)/C_{lipid}(t)$ were plotted against time, and k_{uptake} and $K_{PDMS/lipid}$ were fitted with eq. 9.

$$\frac{C_{PDMS}}{C_{lipid}}(t)=K_{PDMS/lipid}\times\left(1-e^{-k_{uptake}\times t}\right) \quad (9)$$

***In vitro* bioassay.** The extraction method is ultimately aimed at extracting complex mixtures from tissue for analysis with *in vitro* bioassays. Therefore, uptake kinetic experiments from liver tissue in PDMS were conducted with PCB126 as bioactive hydrophobic model chemical, which acts as agonist in the AhR CALUX (chemically activated luciferase expression) bioassay.[46-48] Homogenized liver tissue was spiked with PCB126 at concentrations of 240 - 570 $ng_{PCB126}\ g_{liver}^{-1}$ and passive sampling was carried out statically as well as dynamically with the described stirrer. The concentrations of PCB126 were quantified in the extracts with GC-MSD (Text S6) and the extracts were submitted to the AhR CALUX *in vitro* bioassay for the activation of the aryl hydrocarbon receptor (AhR) assay (Text S7).

RESULTS AND DISCUSSION

Determination of the lipid, protein and water content. Total lipids were determined gravimetrically after solvent extraction. Solvent and negative controls gave a low background signal with 0.1% of weight extracted, which was used for blank subtraction. Positive controls showed good recoveries with an extraction efficacy between 99.1% for triolein and 99.8% for 1-palmitoyl-2-oleoyl-sn-glycero-3-phosphocholine.

The tissues had lipid contents ranging from 3.14 to 809 $g_{lipid}\ kg_{tissue}^{-1}$ after blank subtraction and correction for recovery of the positive controls (Table 1). Total protein content of the tissue samples ranged

from 16.2 to 160 $g_{protein}$ kg_{tissue}^{-1} (Table 1). The measured total water content ranged between 130 and 787 g_{water} kg_{tissue}^{-1} (Table 1). These protein and lipid contents agree well with data for human tissues,[33] assuring that we can use pork tissue as a model for method development and apply it later to human tissue.

Table 1. Total Lipid, Protein and Water Content of Liver, Brain and Adipose Tissue as well as Blood.

tissue	total lipid content m_{lipid} m_{tissue}^{-1} (SD)[a] (g_{lipid} kg_{tissue}^{-1}) (n=3)	total protein content $m_{protein}$ m_{tissue}^{-1} (SD)[a] ($g_{protein}$ kg_{tissue}^{-1}) (n=3)	total water content m_{water} m_{tissue}^{-1} (SD)[a] (g_{water} kg_{tissue}^{-1}) (n=5)
pork adipose tissue	809.60 (5.14)	16.17 (1.19)	130.22 (2.25)
pork blood	3.14 (0.04)	160.37 (5.17)	787.02 (0.36)
pork liver tissue	39.73 (0.75)	157.07 (4.80)	732.93 (2.30)
pork brain tissue	105.02 (0.64)	60.90 (2.34)	783.89 (4.14)

[a]SD: standard deviation.

Coextraction of lipids into PDMS. The PDMS weight gained during the experiments was recorded for each PDMS disk or strip and is reported in Tables S6, S7, S9 and S11 as "m_{PDMS} +Δm_{PDMS} [mg]" and "co-extracted lipid [%]", which is Δm_{PDMS}/ m_{PDMS}. The percentage of co-extracted lipid was dependent on the exposure time (Figure 2A) presumably due to the lipids physically entering the pores of the PDMS because the weight gain was highest for the adipose tissue followed by liver, brain and blood. Weight gain was 0.06 ± 0.03% (n=38, CV 49%) for blood, which is negligible and did not show any time-dependence. The low weight gain was consistent with previously observed 0.013% weigh gain in turtle blood.[21] The low weight gain confirmed our initial assumption that proteins are not taken up into PDMS. Blood proteins adsorb to PDMS,[49] but the surface was wiped rigorously with dry and wet tissues prior to solvent extraction of PDMS and that should remove the proteins or anything adsorbed to the surface.

In adipose tissue, the time to reach 95% of steady state, t_{95}, was 18 h (Figure 2A) with an overall weight gain of 0.70 ± 0.07% (n=36, CV 11%) after t_{95} (Figure 2B). The weight gain of adipose tissues corresponded to earlier work on dugong blubber with 0.6% weight gain.[23] In brain, the time to reach 95% of steady state t_{95} was 12 h (Figure 2A) with an overall weight gain of 0.16 ± 0.04% (n=33, CV 26%) after t_{95} (Figure 2B). It has been shown that pure medium-chain triglyceride oils can let silicone used for gastrostomy feeding tubes swell by 3%, while liquid feeding formula with smaller fractions of medium-chain triglyceride oils absorbed a similar range as the pork fat (0.2 to 1.2%).[50] Adipose tissue is mainly composed of pure triacyl glycerides, whereas brain lipids are 55% phospholipids,[33] which are likely not to be taken up into silicone, which could explain the much reduced weight gain for brain tissue.

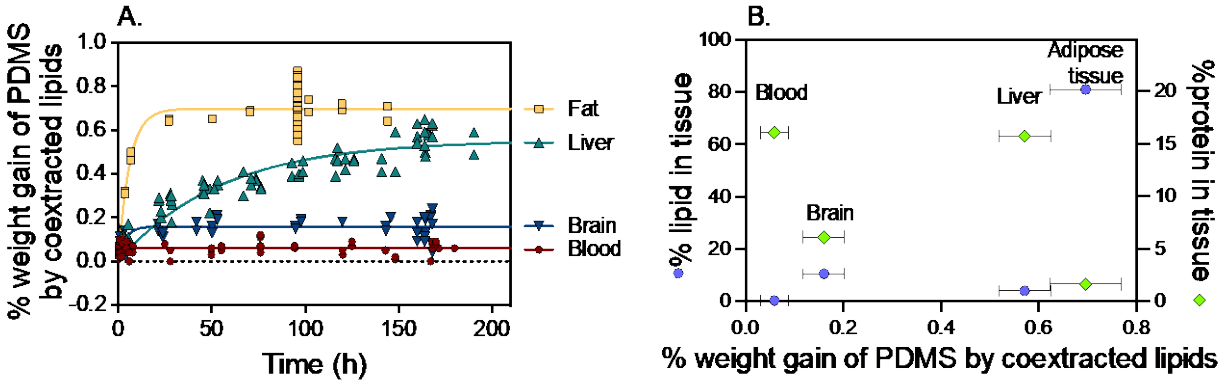

Figure 2. (A) Uptake of lipid into PDMS as a function of time described by weight gain of each individual PDMS disk or strip given Tables S6, S7, S9 and S11. (B) Relationship between % weight gain of PDMS by coextracted lipids and the lipid and protein content of the four different tissues.

The slow kinetics with t_{95} of 165 h (Figure 2A) and a large weight gain of liver with 0.57 ± 0.05% (SD, n=15, CV 9%) despite the lower lipid content came as a surprise. Liver had a very similar protein content as blood (Table 1) but behaved very differently (Figure 2B). One big difference to brain was that the protein content is much higher for liver (Table 1). Since proteins form a surface layer on PDMS within one hour,[51] the diffusion through this layer might have delayed the uptake of lipids into the PDMS because even after 180 h, there was still an upward trend observed (Figure 2A). In addition, although the lipid content of liver was 2.5 times lower than of brain, the liver is expected to have only 30% of its lipid as neutral lipids and 70% as phospholipids (10% even as acidic phospholipids).[33] Zwitterionic and charged phospholipids are unlikely to be taken up into the PDMS. Support for this assumption gives the observation that the large and charged proteins not being able to penetrate PDMS because no weight gain was observed in the protein-rich blood. In addition, partitioning of ionizable organic chemicals to PDMS is dependent solely on the partitioning of the neutral species.[52] Experiments with silicone feeding tubes showed that pure triacylglyceride oils were taken up into the silicone tubes more readily than formulations with other nutrients.[50]

Partitioning from adipose tissue to PDMS. Adipose tissue (Table S6, see also comments on analytical problems with certain compounds in this table) reached equilibrium very fast, so that no uptake kinetic curves were prepared but the ratios C_{lipid}/C_{PDMS} of all individual measurements at t > 50 h were averaged to obtain the $K_{lipid/PDMS}$. It was confirmed that steady state had been reached within 96 h in the static extraction set-up by applying different thicknesses of PDMS according to Reichenberg et al.[53] and Jahnke et al.[24] as described in Text S8 and Figure S5.

The $K_{lipid/PDMS}$ for the pork adipose tissue (Table 2) were calculated from concentrations in extracts using the MBM with eqs. 3 to 5. The chemical fraction bound to protein and remaining in water was

negligible even for very hydrophilic chemicals, thus, effectively we had to correct only for coextracted lipids, which becomes an important correction term if $K_{lipid/PDMS} > 50$. The condition of negligible depletion ($n_{PDMS} < 5\%\ n_{tot}$) was met for most chemicals with a few exceptions (diazinon, metolachlor, TCEP). For consistency, we still performed the calculations with the complete MBM.

The $K_{lipid/PDMS}$ for the POPs agreed within a factor of two with $K_{lipid/PDMS}$ from literature determined with various oils,[54] fish oil[55] and corn oil[56] (Figure 3A). Passive sampling of adipose tissue with PDMS has been performed for a long time and partition constants were typically calculated from the concentrations in lipids quantified after solvent extraction of the tissue followed by acid digest clean-up and the concentrations in PDMS quantified after solvent extraction. Method comparison is only possible for POPs because degradable chemicals would be lost during lipid removal, but the good agreement with literature confirms that the MBM is valid.

The $K_{lipid/PDMS}$ obtained from the PDMS extract using the MBM were subsequently converted to $K_{lipid/water}$ with the $K_{PDMS/water}$ in Table 2. The resulting $\log K_{lipid/water}$ (Table S1) correlated linearly with $\log K_{ow}$ (Figure 3B), extending the existing linear regression for hydrophobic chemicals to the hydrophilic region towards $\log K_{ow}$ of 2.

The $\log K_{lipid/water}$ of the pork adipose tissue also agreed well with the literature data, which were evidently covering the upper end of the hydrophobicity scale (Figure 3C). For comparison, the storage lipid-water partition constant was also predicted with a LSER (Table S1).[57]The experimental $\log K_{lipid/water}$ lay generally within a factor of ten within the predicted values.

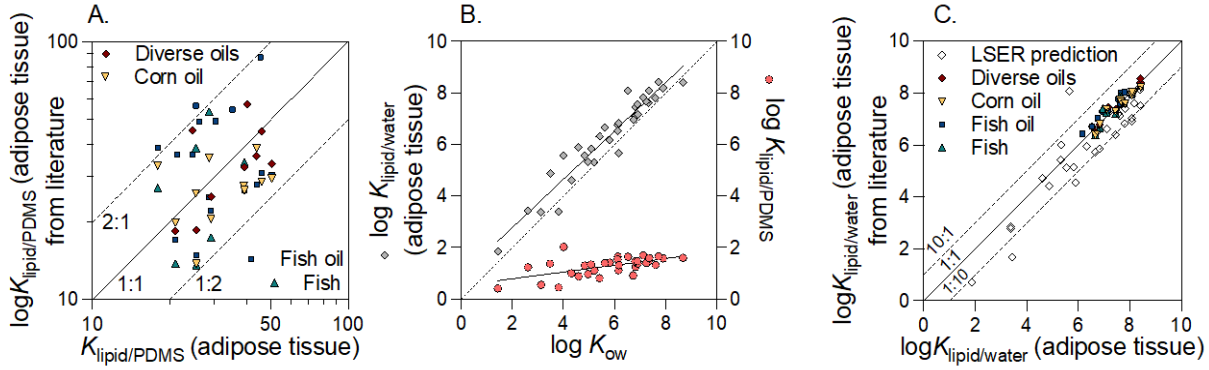

Figure 3. (A) Comparison of the $\log K_{lipid/PDMS}$ of the pork adipose tissue quantified with the MBM with $\log K_{lipid/PDMS}$ from the literature. (B) Correlation of $\log K_{lipid/water}$ with $\log K_{ow}$ (line: $\log K_{lipid/water} = 0.94 \log K_{ow} + 0.90$, $r^2 = 0.914$) and of $\log K_{lipid/PDMS}$ with $\log K_{ow}$ (line: $\log K_{lipid/PDMS} = 0.13 \log K_{ow} + 0.53$, $r^2 = 0.35$). (C) $\log K_{lipid/water}$ of the pork adipose tissue in comparison with $\log K_{lipid/water}$ from literature (mean of diverse oils,[54] corn oil,[56] fish oil [29, 58] and fish[55]) and predictions using the LSER from Geisler et al.[57]

Despite the chemicals covering eight orders of magnitude of hydrophobicity expressed by logK_{ow} or log$K_{lipid/water}$, the log$K_{lipid/PDMS}$ only shows a small hydrophobicity dependence (Figure 3B, right y-axis) with a mean $K_{lipid/PDMS}$ of 18 (95% CI 14 to 25, mean drawn from log$K_{lipid/PDMS}$, therefore the CI is asymmetric with respect to $K_{lipid/PDMS}$). Most of the $K_{lipid/PDMS}$ experiments have used oil or fish. Dugong blubber, which is of similar consistency as pork adipose tissue, yielded consistent $K_{lipid/PDMS}$ with dioxins having a median $K_{lipid/PDMS}$ of 30 if there was no correction for uptake of lipids done,[23] and 38 if one accounted for uptake of 0.6% lipids into PDMS.[26]

Table 2. Octanol-Water Partitioning Constant Log K_{ow} and PDMS-Water Partitioning Constant Log $K_{PDMS/water}$ from Literature and Measured Partition Constants $K_{lipid/PDMS}$ for Each Tissue.

chemical	abbreviation	CAS	log K_{ow}[a]	log $K_{PDMS/water}$	adipose tissue $K_{lipid/PDMS}^{m,n}$ (SE)[o]		liver tissue $K_{lipid/PDMS}^{p,n}$ (SE)[o]		brain tissue $K_{lipid/PDMS}^{p,n}$ (SE)[o]	
mean (95% CI) of all chemicals (from mean of log $K_{lipid/PDMS}$)					**18 (14-25)**		**15 (10-21)**		**3.8 (2.6-5.4)**	
aldrin	aldrin	309-00-2	6.50	5.49[b]	n.d		13.0	0.7	1.9	0.2
atrazine	atrazine	1912-24-9	2.61	2.18[c]	16.7	1.1	4.5	0.1	1.6	0.1
benzo[*a*]pyrene	B[*a*]P	50-32-8	6.13	5.09[d]	42.4	3.1	56.1	2.2	84.0	5.0
2,4,4'-tribromodiphenyl ether	BDE28	41318-75-6	5.94	5.43[e]	n.d		8.2	0.3	2.5	0.3
2,2',4,4'-tetrabromodiphenyl ether	BDE47	5436-43-1	6.81	5.84[e]	16.7	1.0	19.0	0.7	3.5	0.3
2,2',4,4',5-pentabromodiphenyl ether	BDE99	60348-60-9	7.32	6.17[e]	26.7	1.7	40.6	2.7	6.2	0.8
2,2',4,4',6-pentabromodiphenyl ether	BDE100	189084-64-8	7.24	6.25[e]	23.7	1.7	42.6	2.6	6.2	0.6
2,2′,4,4′,5,5′-hexabromodiphenyl ether	BDE153	68631-49-2	7.90	6.60[e]	36.7	2.6	90.1	55.4	24.6	4.0
bromophos-ethyl	bromophos-E	4824-78-6	6.15	4.54[f]	12.7	0.7	7.2	0.3	2.6	0.2
bromophos-methyl	bromophos-M	2104-96-3	5.21	4.20[f]	12.5	0.4	5.6	0.2	2.7	0.2
chlorfenapyr	chlorfenapyr	122453-73-0	4.83	4.25[g]	16.7	0.9	6.0	0.2	1.8	0.1
chrysene	chrysene	218-01-9	5.81	4.74[d]	23.9	1.5	23.5	0.7	37.5	2.2
chlorpyrifos	chlorpyrifos-E	2921-88-2	4.96	4.36[h]	9.1	0.3	3.9	0.1	2.0	0.1
chlorpyrifos-methyl	chlorpyrifos-M	5598-13-0	4.31	3.61[f]	9.8	0.3	4.5	0.1	2.0	0.1
cybutryne (irgarol)	cybutryne	28159-98-0	3.48	3.50[h]	22.6	2.7	5.8	0.2	2.9	0.2
diazinon	diazinon	333-41-5	3.81	2.93[f]	2.8	0.1	1.0	0.1	0.8	0.1
p,p'-dichlorodiphenyldichloroethane	*p,p'*-DDD	72-54-8	6.12	4.98[i]	33.9	1.5	8.8	0.3	2.5	0.1
p,p'-dichlorodiphenyldichloroethylene	*p,p'*-DDE	72-55-9	6.73	6.04[i]	8.0	0.3	10.0	0.4	2.2	0.2
p,p'-dichlorodiphenyltrichloroethane	*p,p'*-DDT	50-29-3	6.91	5.79[i]	19.0	1.2	38.7	2.3	3.2	0.2
p,p'-dimethoxydiphenyltrichloroethane	methoxychlor	72-43-5	5.08	4.49[h]	21.3	0.9	13.1	0.5	2.4	0.2
etofenprox	etofenprox	80844-07-1	7.05	6.09[g]	n.d		18.1	1.0	2.0	0.2
fipronil	fipronil	120068-37-3	4.00	3.56[g]	90.4	6.5	64.0	2.4	11.2	0.4
γ-hexachlorocyclohexane	lindane	58-89-9	3.72	2.99[i]	n.d		10.6	0.3	3.1	0.2
heptachlor	heptachlor	76-44-8	6.1	5.57[b]	n.d		11.6	0.5	2.1	0.1

chemical	abbreviation	CAS	log K_{ow}[a]	log $K_{PDMS/water}$	adipose tissue $K_{lipid/PDMS}$[m,n]	(SE)[o]	liver tissue $K_{lipid/PDMS}$[p,n]	(SE)[o]	brain tissue $K_{lipid/PDMS}$[p,n]	(SE)[o]
metolachlor	metolachlor	51218-45-2	3.13	2.82 [h]	3.4	0.1	1.0	0.1	0.6	0.1
2,4,4'-trichlorobiphenyl	PCB28	7012-37-5	5.62	5.25 [i]	24.6	0.7	4.7	0.2	2.3	0.1
2,2′,5,5′-tetrachlorobiphenyl	PCB52	35693-99-3	6.17	5.52[i]	20.4	0.7	7.7	0.3	2.1	0.1
2,2′,4,5,5′-pentachlorobiphenyl	PCB101	37680-73-2	6.80	5.99 [i]	28.1	1.1	13.1	0.6	2.2	0.2
2,3,4,4',5-pentachlorobiphenyl	PCB114	74472-37-0	6.65	6.07 [i]	n.d.		13.5	0.7	3.7	0.3
2,3',4,4',5-pentachlorobiphenyl	PCB118	31508-00-6	7.12	6.11 [i]	48.3	1.7	14.0	0.7	2.8	0.3
3,3',4,4',5-pentachlorobiphenyl	PCB126	57465-28-8	6.89	6.08 [i]	30.2	2.8	16.8	0.9	3.8	0.4
2,2′,3,4,4′,5′-hexachlorobiphenyl	PCB138	35065-28-2	7.35	6.49 [i]	37.8	1.4	25.4	1.5	2.9	0.7
2,2′,4,4′,5,5′-hexachlorobiphenyl	PCB153	35065-27-1	6.53	6.45 [i]	42.2	1.6	31.4	2.1	3.4	0.6
2,3,3',4,4',5-hexachlorobiphenyl	PCB156	38380-08-4	7.60	6.47 [i]	21.4	2.0	32.5	2.0	6.4	0.9
2,2′,3,4,4′,5,5′-heptachlorobiphenyl	PCB180	35065-29-3	7.72	6.76 [i]	50.2	3.2	65.9	5.5	6.7	1.9
2,2',3,3',4,4',5,5'-octachlorobiphenyl	PCB194	35694-08-7	8.68	6.79 [j]	32.3	2.1	53.4	33.2	19.7	3.4
decachlorobiphenyl	PCB209	2051-24-3	8.27	7.81 [k]	n.d		198	91	67.0	8.2
tris(2-chloroethyl) phosphate	TCEP	115-96-8	1.44	1.44 [g]	2.6	0.1	71.9	4.3	15.0	0.9
tris(ortho-methylphenyl) phosphate	TMPP	78-30-8	5.41	5.50 [l]	6.3	0.2	3.5	0.1	1.1	0.1
triphenyl phosphate	TPP	115-86-6	4.59	4.94 [l]	7.5	0.4	n.d		0.9	0.1

[a]Experimental data from PhysPropNCCT.[59] [b]Data from Heltsley et al.[60] [c]Data from Magnér et al.[61] [d]Data from Kwon et al.[62] [e]Data from Endo et al.[63] [f]Data from UFZ LSER database[41] [g]Data predicted with own QSAR: log $K_{PDMS/water}$ = 0.8291 log K_{ow} + 0.2454. [h]Data from Neale et al.[64] [i]Data from Smedes et al[65] [j]Data from Hsieh et al.[66] [k]Data from Yates et al.[67] [l]Data from Pintado-Herrera et al.[68] [m]From average of all experimental data >50 h for adipose tissue (Table S6). [n]The $K_{lipid/PDMS}$ were corrected for coextracted lipids. [o]SE: standard error. [p]From fit of the uptake kinetics in liver and brain (Tables S9 and S11). N.d.: not determined.

Partitioning from blood to PDMS. The initial idea was to keep a similar experimental design for pork blood with approximately 400 mg PDMS and 2.2 mL of blood, guided by the previous design for turtle blood.[21] However, depletion was larger than predicted (Table S7; any analytical issues are indicated in this table), so the PDMS exhaustively extracted 15 of 40 test chemicals, for which no $\log K_{blood/PDMS}$ could be established. For these 15 chemicals, a mean ratio of $n_{extract}/n_{tot}$ of 1.2 ±0.4 was obtained, indicating that loss processes were negligible.

It was possible to establish the uptake kinetics by plotting $n_{extract}/n_{tot}$ as a function of time (Figure S6). The t_{95} increased with hydrophobicity of the chemicals (Figure S7) and ranged from less than an hour to 50 h for most chemicals up to $\log K_{ow}$ of 7 (Table S8). T_{95} was 88 h for PCB153 and the very hydrophobic BDE153, PCB180 and PCB194 exceeded the 100 h.

All data, for which depletion was lower than 80% and t > 50 h, were averaged to derive $\log K_{blood/PDMS}$ for 26 chemicals (Table S8). The $\log K_{blood/PDMS}$ varied quite a bit due to the high depletion observed but was essentially independent of the hydrophobicity (Figure 4) with a mean of 16 g_{PDMS}/g_{blood} (95% CI 11 to 21). The 14 chemicals, for which no $K_{blood/PDMS}$ could be derived due to too high depletion, covered the entire hydrophobicity range as marked by the empty circles on the x-axis in Figure 4. The $\log K_{PDMS/\ blood}$ were in the same range as previous measurements with turtle blood[21] (Figure S8) but covered a much higher range of hydrophobicity than in previous studies.

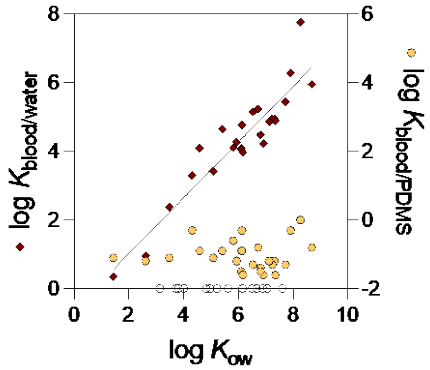

Figure 4. Independence of the $\log K_{blood/PDMS}$ ($g_{PDMS}\ g_{blood}^{-1}$) from hydrophobicity expressed as the $\log K_{ow}$ (right y-axis) and correlation of the $\log K_{ow}$ with $\log K_{blood/water}$ (calculated by multiplying the $K_{blood/PDMS}$ (Table S8) by the $K_{PDMS/water}$ (Table 1) assuming a density of 1 L kg^{-1} for, both, blood and water) (left y-axis). Empty circles on the x-axis mark the chemicals that were fully depleted and for which no $K_{blood/PDMS}$ could be derived. The regression line (black line) is $\log K_{blood/water} = 0.81 \log K_{ow} - 0.61$, $r^2 = 0.8583$, $S_{y,x} = 0.5753$, F = 145.

The $K_{lipid/PDMS}$ for the blood lipids were calculated with eq.7 and are listed in Table S8. They were in the same range as for adipose tissue (Figure 5A). The $K_{lipid/PDMS}$ for blood are subject to high uncertainty because they were measured under close to depletive conditions but even under these conditions, the values are

remarkably close to each other considering that adipose tissue contained 81% lipid and blood only 0.3% lipid (Table 1), confirming the wide applicability of the mass-balance approach.

Partitioning from liver tissue to PDMS. A few of the more hydrophobic chemicals met negligible-depletion conditions but for most there was a substantial depletion by partitioning to PDMS (Table S9, any analytical issues that led to omission of some datapoints are indicated in the table) and the MBM (eqs. 3 and 4) was used to derive the ratios $C_{PDMS}(t)/C_{lipid}(t)$ (Table S9). The uptake kinetics are shown in Figure S6. The time to reach 95% completion of extraction $t_{95\%}$ ranged from 7 h to over 200 h (Table S10), log-linearly increasing with hydrophobicity (Figure S7), but most chemicals with exception of PCB180, PCB194 and PCB209 came close to steady state in the 190 h of the experiment. The tissue cannot be kept much longer than 8 days because it starts to decay despite performing the extraction at 4 - 8 °C. The $K_{lipid/PDMS}$ (Table 2) were in a similar range as for blood and adipose tissue.

The similarity of $K_{lipid/PDMS}$ between tissues also indicates that no substantial metabolic degradation occurred in the liver tissue despite its principally higher metabolic activity than adipose or brain tissue. The metabolic activity of liver tissue is typically lost within hours after sampling as experience with rat liver S9 fractions indicates. Most of the spiked chemicals are relatively stable. The phosphate esters are likely to be metabolizable but only triphenylphosphate could not be recovered in the PDMS extracts of the liver (Table S9).

If there had been substantial degradation, the $K_{lipid/PDMS}$ would have been overestimated by the MBM approach because the true C_{lipid} would have been smaller than if the concentration was constant over the sampling time. Apart from TCEP, which had a substantially higher $K_{lipid/PDMS}$ in liver and brain than in adipose tissue, where it fell on the regression line in Figure S9, no other chemicals showed such a pattern, not even the phosphate TMPP or any of the organothiophosphate insecticides, which are also easily oxidized or hydrolyzed by liver enzymes.

Partitioning from brain tissue to PDMS. The uptake kinetics from brain tissue to PDMS (Table S11 and Figure S6) showed $t_{95\%}$ ranging from 8 – >200 h (Table S12) and were remarkably similar to liver (Figure S7) despite a factor of ten higher in lipid content in the brain tissue. The protein content was very similar in both tissues, and it can be envisaged that the proteins might also facilitate transport.[69] The $K_{lipid/PDMS}$ (Table 2) were in the same range as the other tissues (Figure 5A).

Comparison of lipid-PDMS partitioning for the different tissue and role of correction for lipid uptake. The $K_{lipid/PDMS}$ (Table 2) overlapped in all tissues and blood and did not show any strong dependence on the $\log K_{ow}$ (Figure 5A). Overall, they varied within a tissue as much as between tissues. However, as seen for

adipose tissue, liver and brain also showed a slight increase in $K_{lipid/PDMS}$ with hydrophobicity (Figure S9) but the slope was very small (slope 0.13 for adipose tissue, 0.16 for liver tissue and 0.10 for brain tissue) and within the variability of the measurements.

The log$K_{lipid/PDMS}$ was 1.26 (95% CI 1.13 – 1.39) for adipose tissue, 1.16 (1.00 – 1.33) for liver and 0.58 (0.42 – 0.73) for brain tissue with individual $K_{lipid/PDMS}$ and the non-logarithmic means and confidence intervals listed in Table 2. These log$K_{lipid/PDMS}$ are corrected for uptake of lipids and the average had to be drawn for the logarithmic values for equivalency of the mean values considering log$K_{lipid/PDMS}$ = -log $K_{PDMS/lipid}$.

Finally, while we report here $K_{lipid/PDMS}$ or $K_{PDMS/lipid}$ for the pure PDMS after correction for uptake of lipids into PDMS, when passive sampling is applied in practise for testing the passive sampling extracts in *in vitro* bioassays, the coextracted lipid is in the PDMS extract and will be dosed into the bioassay. For this purpose, the $K_{PDMS+coextracted\ lipid/lipid}$ must be calculated with eq.10 with fractions of coextracted lipids measured in each specific experiment. The resulting $K_{lipid/PDMS+coextracted\ lipid}$ were 16 for adipose tissue, 13 for liver and 3.8 for brain tissue using the fractions of coextracted lipids measured in the present study (Figure 2B).

$$K_{PDMS+coextracted\ lipid/lipid} = \frac{m_{PDMS}}{m_{PDMS}+\Delta m_{PDMS}} \times K_{PDMS/lipid} + \frac{\Delta m_{PDMS}}{m_{PDMS}+\Delta m_{PDMS}} \quad (10)$$

Comparison of lipid-water partitioning of the different tissue. The $K_{lipid/PDMS}$ (Table 2) were converted to $K_{lipid/water}$ by multiplication with the $K_{PDMS/water}$ (Table S1) using Hess' law (eq. 11).

$$K_{lipid/water} = K_{lipid/PDMS} \times K_{PDMS/lipid} \quad (11)$$

The resulting $K_{lipid/water}$ (Tables S1 (adipose tissue), S8 (blood), S10 (liver), S12 (brain)) ranged over seven orders of magnitude but varied little between the different tissues, with all of them within a factor of ten from the K_{ow} (Figure 5B), thus agreeing well with literature data of $K_{lipid/water}$. There seems to be a small but systematic deviation from the 1:1 line with adipose tissue having slightly higher and brain tissue having slightly lower $K_{lipid/water}$, but this systematic deviation might also be an artifact from the uncertainty of the lipid determination, given the vastly different lipid contents of the different tissues.

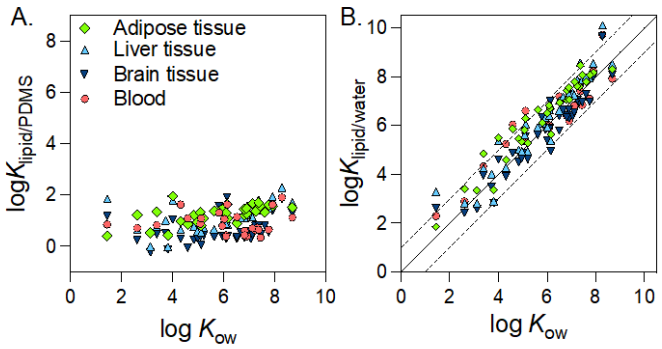

Figure 5. (A) Comparison of log$K_{lipid/PDMS}$ (Table 2) between the tissues and independence of logK_{ow}. (B) Comparison of log$K_{lipid/water}$ between the tissues (Tables S1 (adipose tissue), S8 (blood), S10 (liver), S12 (brain)) and correlation with logK_{ow} (Table 2). The drawn lines are the 1:1 line and the broken lines correspond to ± one log unit.

Uncertainties related to the MBM approach. The MBM relies upon the equilibrium being attained so that thermodynamic calculations can be made. Within the practically feasible extraction time frame of approximately 200 h, chemicals up to a logK_{ow} of 8 reached 95% of equilibrium (Figure S7), which means that the concentrations of chemicals with logK_{ow} > 8 would be underestimated when using the experimental set up for brain and liver, while adipose tissue and blood were not impacted by this limitation.

The derived $K_{lipid/PDMS}$ appear to be rather robust and ranged within a factor of two from literature in case of adipose tissue (Figure 3A) but one needs to be mindful that the literature data have as much inherent variability even if they were measured with pure lipids. When converting $K_{lipid/PDMS}$ to $K_{lipid/water}$, one also needs $K_{PDMS/water}$ (Table S1) and these depend very much on the type of silicone[65] and are difficult to measure for very hydrophobic chemicals.[62]

The MBM provides a way to deal with hydrophilic and hydrophobic neutral organic chemicals with one common approach. This is novel: so far, concentrations in PDMS have only been converted directly to lipid concentrations without considering chemicals in proteins and water, which become relevant in lipid-poor tissue and for more hydrophilic chemicals. However, the MBM requires partition constants between lipid and water as well as between protein and water. There is only limited availability of experimental partition constants and the typically used lipid surrogates are storage lipids and membrane lipids and the typically used protein surrogates are serum albumin and chicken breast muscle proteins. These surrogates alone differ substantially in their numerical K values (Figure S10A for $K_{lipid/water}$ and Figure S10B for $K_{protein/water}$) and the available data for the chemicals included in this study were only partially experimental data, many were predicted by LSERs (Table S1), which adds to the uncertainty.

The most influential parameter for the outcome of the MBM is the $K_{lipid/protein}$. A $K_{lipid/protein}$ of 20 was derived from QSAR models in the literature as described above. The $K_{lipid/protein}$ from the various types of $K_{lipid/water}$ and $K_{protein/water}$ (Figure S10C) varied between chemicals and the 95% confidence intervals of $K_{lipid/protein}$ ranged from 8 to 65 for the different combinations of $K_{lipid/water}$ and $K_{protein/water}$. The $K_{lipid/protein}$ were much higher if muscle proteins were used as surrogate than when serum proteins were used. The type of lipid mattered little. Despite these uncertainties and variability, the MBM is still a big step forward because it allows the application of passive equilibrium sampling under depletive conditions and for a much wider range of tissue types and chemicals than any previous method.

Application of the extracts to bioassays. To assess the suitability of the PDMS extraction method as a sample preparation for *in vitro* bioassays, we spiked liver tissue with PCB126 and recorded the uptake kinetics both in the static and stirred sampling experiments in liver tissue by chemical analysis and the AhR CALUX.

The concentration of PCB126 in PDMS (Table S13) reached equilibrium within 80 hours in the stirred set up but had not even reached 50% of equilibrium under static conditions (Figure 6A, left y-axis). The same uptake kinetics were observed with bioanalytical equivalent concentrations (PCB126-EQ) from the AhR CALUX assay (Figure 6 A, right y-axis). Measured concentrations of chemical (PCB126, blue) and bioanalytical (PCB126-EQ, orange) analysis were in good agreement (Figure 6B), indicating that the measured concentrations of PCB126 could be confirmed with the AhR CALUX assay (ratio of PCB126-EQ/PCB126 between 0.6 and 1.4) and that the extracts can be used in *in vitro* bioassays.

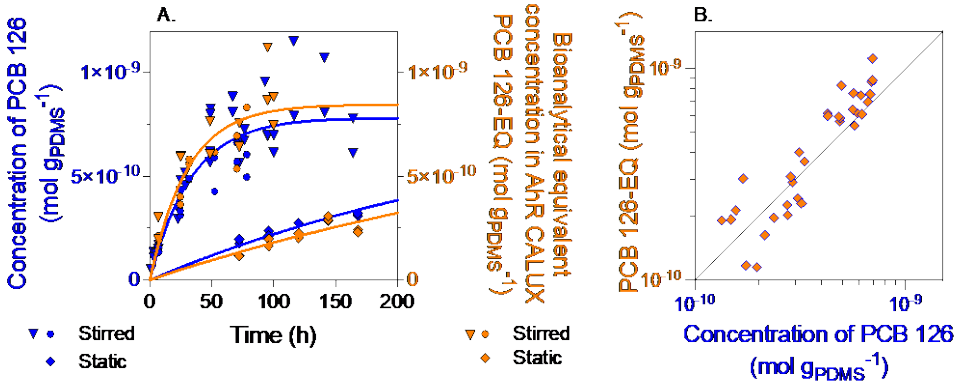

Figure 6. A. Comparison of uptake kinetic experiments of PCB126 from lean liver tissue homogenate into PDMS measured with GC (blue) and AhR CALUX (orange) in both static and stirred experimental set-ups. Results are expressed as the concentration of PCB126 in PDMS [mol g_{PDMS}^{-1}] from chemical analysis and bioanalytical equivalent concentration (PCB126-EQ) [mol g_{PDMS}^{-1}] from the AhR CALUX bioassay. B. Direct comparison of concentration of PCB126 with PCB126-EQ. The line is the 1:1 line. Data are in Table S13.

In Figure 6, no correction of coextracted lipids was performed, because in practice the whole extract is dosed to the bioassay and one can account for the effect of the coextracted lipid by using the $K_{\text{lipid/PDMS+coextracted lipid}}$ to convert the concentration in the PDMS extract to lipid-normalized tissue concentrations, which is 13 for liver as derived above.

Alternatively, one can use eq.11 to estimate the role of coextracted lipids to the extracted amount of PCB126. Correction for coextraction of lipid during passive sampling would lead to a C_{PDMS} that is 0.8 – 9.7% lower than by using the total extract in the calculation.

$$C_{PDMS} = \frac{n_{extract}}{m_{PDMS}} / \left(1 + \frac{K_{lipid/PDMS} \times \Delta m_{PDMS}}{m_{PDMS}}\right) \quad (11)$$

There is one caveat, though, when the extract with the coextracted lipid is dosed into bioassays, there is also partitioning between the co-dosed lipid and the bioassay medium and the overall sensitivity of the bioassay is decreased in comparison to dosing the same amount of extract but without co-dosed lipid.[48] As Figure 6B demonstrates, there is little difference in analytically measured PCB126 concentrations and its bioanalytical equivalents PCB126-EQ but this can change in samples with lower levels of contamination, where a non-negligible amount of lipid is dosed to the bioassay.[48]

Recommendations for unbiased extractions of mixtures of organic chemicals. Passive equilibrium sampling has been applied so far only to tissue sampling of POPs, but we were able to demonstrate that the range of applicability can be extended to cover eight orders of magnitude of hydrophobicity expressed by $\log K_{ow}$ with very little difference in extraction efficiency expressed by $\log K_{PDMS/lipid}$ or $\log K_{PDMS/tissue}$. Coextracted lipids were negligible for blood, < 0.6% for liver, < 0.2% for brain and < 0.7% for adipose tissue, permitting chemical analysis in *in vitro* bioassays without any further clean-up. Kinetics were fast with adipose tissue, where the experiments could even be performed under static conditions, and with blood that could easily be agitated, either with a stirrer or by rolling the vials. For adipose tissue sampling is typically non-depletive because one needs approximately a ratio of 3:1 of adipose tissue to PDMS to physically cover the PDMS disks. Even if that ratio could be decreased to 1:1, sampling would remain non-depletive. This is no problem, provided that the detection limits are low enough and the small fraction of coextracted lipid does not interfere with the bioassays.[48]

Extraction of blood was depletive for many chemicals and since uptake kinetics into PDMS are fast, our suggestion is to increase the ratio PDMS to blood as much as practically feasible to be fully depletive for all chemicals. This is also recommended because blood is the matrix with the lowest level of contamination. However, exhaustive extraction (>90% depletion) would require 3 g of PDMS per 1 g of blood, which is logistically almost impossible. If only very small quantities of blood in the microliter range are available, pipetting it on top of PDMS and potentially sandwiching with another PDMS sheet might be an option to

further explore. Overall, it is possible to reliably extract mixtures of organic chemicals without changing the composition from a very wide range of tissue which gives opportunities for biomonitoring and direct comparison of different tissues in physiologically based pharmacokinetic modelling and other applications.

ASSOCIATED CONTENT

Supporting Information

The supporting information is available free of charge at https://pubs.acs.org/doi....

All experimental data. (XLSX)

Additional information on the experiments, uptake kinetics, comparison of results with literature. (PDF)

AUTHOR INFORMATION

Corresponding Author

Beate I. Escher − UFZ − Helmholtz Centre for Environmental Research, Leipzig 04318, Germany; orcid.org/0000-0002-5304-706X; Email: beate.escher@ufz.de

Authors

Andreas Baumer – *Department Cell Toxicology, Helmholtz Centre for Environmental Research– UFZ, 04318 Leipzig, Germany*

Sandra Jäsch – *Department Analytical Environmental Chemistry, Helmholtz Centre for Environmental Research– UFZ, 04318 Leipzig, Germany*

Nadin Ulrich – *Department Analytical Environmental Chemistry, Helmholtz Centre for Environmental Research– UFZ, 04318 Leipzig, Germany*

Ingo Bechmann – *Institute of Anatomy, University of Leipzig, 04103 Leipzig, Germany*

Julia Landmann – *Institute of Anatomy, University of Leipzig, 04103 Leipzig, Germany*

Beate I. Escher – *Department Cell Toxicology, Helmholtz Centre for Environmental Research– UFZ, 04318 Leipzig, Germany and Eberhard Karls University Tübingen, Environmental Toxicology, Centre for Applied Geosciences, 72076 Tübingen, Germany*

Author Contribution

A.B. planned and performed the experiments and evaluated the data. S.J. performed a part of the chemical analysis. N.U. helped with analytical method development and study design. B.E. conceived the study and developed all data evaluations and models. I.B. and J.L. contributed to the study design. A.B. and B.E. wrote the manuscript. All authors reviewed the manuscript.

Notes

The authors declare no competing financial interest.

ACKNOWLEDGMENTS

The authors thank Niklas Wojtysiak, Jörg Watzke and Sophia Mälzer for experimental assistance, Peter Portius, Sascha Wagner, Roman Angeli and Nick Hoffmann of the UFZ workshop for building prototypes and the final mixing instruments. We thank Andrea Pfennigsdorff and Darya Gedankina for supporting the GC measurements. Maria König and Lisa Glauch are acknowledged for conducting the AhR CALUX assay including the cell culture. We gratefully acknowledge access to the CITEPro platform (Chemicals in the Environment Profiler) funded by the Helmholtz Association.

REFERENCES

1. United Nations *Stockholm Convention on persistent organic pollutants* United Nations Economic Commission for Europe (UN/ECE), http://chm.pops.int (accessed 10 March 2021): Geneva, Switzerland, and New York, NY, USA, 2009.
2. Escher, B. I.; Stapleton, H. M.; Schymanski, E. L., Tracking complex mixtures of chemicals in our changing environment. *Science* **2020,** *367*, 388-392.
3. Voorspoels, S.; Covaci, A.; Maervoet, J.; De Meester, I.; Schepens, P., Levels and profiles of PCBs and OCPs in marine benthic species from the Belgian North Sea and the Western Scheldt Estuary. *Mar. Pollut. Bull.* **2004,** *49*, 393-404.
4. Gilroy, È. A. M.; Muir, D. G. C.; McMaster, M. E.; Darling, C.; Campbell, L. M.; de Solla, S. R.; Parrott, J. L.; Brown, S. B.; Sherry, J. P., Polychlorinated biphenyls and their hydroxylated metabolites in wild fish from wheatley Harbour Area of Concern, Ontario, Canada. *Environ. Toxicol. Chem.* **2012,** *31*, 2788-2797.
5. Weijs, L.; Dirtu, A. C.; Das, K.; Gheorghe, A.; Reijnders, P. J. H.; Neels, H.; Blust, R.; Covaci, A., Inter-species differences for polychlorinated biphenyls and polybrominated diphenyl ethers in marine top predators from the Southern North Sea: Part 1. Accumulation patterns in harbour seals and harbour porpoises. *Environ. Poll.* **2009,** *157*, 437-444.

6. Weijs, L.; Shaw, S. D.; Berger, M. L.; Neels, H.; Blust, R.; Covaci, A., Methoxylated PBDEs (MeO-PBDEs), hydroxylated PBDEs (HO-PBDEs) and hydroxylated PCBs (HO-PCBs) in the liver of harbor seals from the northwest Atlantic. *Sci. Total Environ.* **2014,** *493*, 606-614.

7. Desforges, J. P.; Eulaers, I.; Periard, L.; Sonne, C.; Dietz, R.; Letcher, R. J., A rapid analytical method to quantify complex organohalogen contaminant mixtures in large samples of high lipid mammalian tissues. *Chemosphere* **2017,** *176*, 243-248.

8. Chu, S. G.; Covaci, A.; Schepens, P., Levels and chiral signatures of persistent organochlorine pollutants in human tissues from Belgium. *Environ. Res.* **2003,** *93*, 167-176.

9. Covaci, A.; de Boer, J.; Ryan, J. J.; Voorspoels, S.; Schepens, P., Distribution of organobrominated and organochlorinated contaminants in Belgian human adipose tissue. *Environ. Res.* **2002,** *88*, 210-218.

10. Guvenius, D. M.; Hassanzadeh, P.; Bergman, A.; Noren, K., Metabolites of polychlorinated biphenyls in human liver and adipose tissue. *Environ. Toxicol. Chem.* **2002,** *21*, 2264-2269.

11. Rappaport, S. M.; Barupal, D. K.; Wishart, D.; Vineis, P.; Scalbert, A., The Blood Exposome and Its Role in Discovering Causes of Disease. *Environ. Health Persp.* **2014,** *122*, 769-774.

12. Pellizzari, E. D.; Woodruff, T. J.; Boyles, R. R.; Kannan, K.; Beamer, P. I.; Buckley, J. P.; Wang, A. L.; Zhu, Y. Y.; Bennett, D. H., Identifying and Prioritizing Chemicals with Uncertain Burden of Exposure: Opportunities for Biomonitoring and Health-Related Research. *Environ. Health Persp.* **2019,** *127*.

13. Anastassiades, M.; Lehotay, S. J.; Stajnbaher, D.; Schenck, F. J., Fast and easy multiresidue method employing acetonitrile extraction/partitioning and "dispersive solid-phase extraction" for the determination of pesticide residues in produce. *J AOAC Int.* **2003,** *86*, 412-431.

14. Baduel, C.; Mueller, J. F.; Tsai, H. H.; Ramos, M. J. G., Development of sample extraction and clean-up strategies for target and non-target analysis of environmental contaminants in biological matrices. *J. Chromatogr. A* **2015,** *1426*, 33-47.

15. Plassmann, M. M.; Schmidt, M.; Brack, W.; Krauss, M., Detecting a wide range of environmental contaminants in human blood samples-combining QuEChERS with LC-MS and GC-MS methods. *Anal Bioanal Chem* **2015,** *407*, 7047-7054.

16. Norli, H. R.; Christiansen, A.; Deribe, E., Application of QuEChERS method for extraction of selected persistent organic pollutants in fish tissue and analysis by gas chromatography mass spectrometry. *J. Chromatogr. A* **2011,** *1218*, 7234-7241.

17. Usui, K.; Hashiyada, M.; Hayashizaki, Y.; Igari, Y.; Hosoya, T.; Sakai, J.; Funayama, M., Application of modified QuEChERS method to liver samples for forensic toxicological analysis. *Forensic Toxicol.* **2014,** *32*, 139-147.

18. Lehotay, S. J.; Mastovska, K.; Yun, S. J., Evaluation of two fast and easy methods for pesticide residue analysis in fatty food matrixes. *J AOAC Int.* **2005,** *88*, 630-638.

19. Chamkasem, N.; Lee, S.; Harmon, T., Analysis of 19 PCB congeners in catfish tissue using a modified QuEChERS method with GC-MS/MS. *Food Chem.* **2016,** *192*, 900-906.

20. Tienpont, B.; David, F.; Desmet, K.; Sandra, P., Stir bar sorptive extraction-thermal desorption-capillary GC-MS applied to biological fluids. *Anal Bioanal Chem* **2002,** *373*, 46-55.

21. Jin, L.; Escher, B. I.; Limpus, C. J.; Gaus, C., Coupling passive sampling with in vitro bioassays and chemical analysis to understand combined effects of bioaccumulative chemicals in blood of marine turtles. *Chemosphere* **2015,** *138*, 292-299.

22. Ossiander, L.; Reichenberg, F.; McLachlan, M. S.; Mayer, P., Immersed solid phase microextraction to measure chemical activity of lipophilic organic contaminants in fatty tissue samples. *Chemosphere* **2008,** *71*, 1502-1510.

23. Jin, L.; Gaus, C.; van Mourik, L.; Escher, B. I., Applicability of Passive Sampling to Bioanalytical Screening of Bioaccumulative Chemicals in Marine Wildlife. *Environ. Sci. Technol.* **2013,** *47*, 7982-7988.

24. Jahnke, A.; Mayer, P.; Broman, D.; McLachlan, M. S., Possibilities and limitations of equilibrium sampling using polydimethylsiloxane in fish tissue. *Chemosphere* **2009,** *77*, 764-770.

25. Jahnke, A.; Mayer, P.; McLachlan, M. S.; Wickstrom, H.; Gilbert, D.; MacLeod, M., Silicone passive equilibrium samplers as 'chemometers' in eels and sediments of a Swedish lake. *Environ. Sci.-Proc. Imp.* **2014,** *16*, 464-472.

26. Jin, L.; Gaus, C.; Escher, B. I., Adaptive Stress Response Pathways Induced by Environmental Mixtures of Bioaccumulative Chemicals in Dugongs. *Environ. Sci. Technol.* **2015,** *49*, 6963-6973.

27. Rusina, T. P.; Carlsson, P.; Vrana, B.; Smedes, F., Equilibrium Passive Sampling of POP in Lipid-Rich and Lean Fish Tissue: Quality Control Using Performance Reference Compounds. *Environ. Sci. Technol.* **2017,** *51*, 11250-11257.

28. Rojo-Nieto, E.; Muz, M.; Koschorreck, J.; Rudel, H.; Jahnke, A., Passive equilibrium sampling of hydrophobic organic compounds in homogenised fish tissues of low lipid content. *Chemosphere* **2019,** *220*, 501-504.

29. Smedes, F.; Sobotka, J.; Rusina, T. P.; Fialova, P.; Carlsson, P.; Kopp, R.; Vrana, B., Unraveling the Relationship between the Concentrations of Hydrophobic Organic Contaminants in Freshwater Fish of Different Trophic Levels and Water Using Passive Sampling. *Environ. Sci. Technol.* **2020,** *54*, 7942-7951.

30. Baumer, A.; Escher, B. I.; Landmann, J.; Ulrich, N., Direct sample introduction GC-MS/MS for quantification of organic chemicals in mammalian tissues and blood extracted with polymers without clean-up. *Anal Bioanal Chem* **2020,** *412*, 7295-7305.

31. Jahnke, A.; Mayer, P.; Schafer, S.; Witt, G.; Haase, N.; Escher, B. I., Strategies for Transferring Mixtures of Organic Contaminants from Aquatic Environments into Bioassays. *Environ. Sci. Technol.* **2016,** *50*, 5424-5431.

32. deBruyn, A. M. H.; Gobas, F. A. P. C., The sorptive capacity of animal protein. *Environ. Toxicol. Chem.* **2007,** *26*, 1803-1808.

33. Schmitt, W., General approach for the calculation of tissue to plasma partition coefficients. *Toxicology in Vitro* **2008,** *22*, 457-467.

34. Endo, S.; Brown, T. N.; Goss, K.-U., General model for estimating partition coefficients to organisms and their tissues using the biological compositions and polyparameter Linear Free Energy Relationships. *Environ. Sci. Technol.* **2013,** *47*, 6630−6639.

35. Quinn, C. L.; van der Heijden, S. A.; Wania, F.; Jonker, M. T. O., Partitioning of Polychlorinated Biphenyls into Human Cells and Adipose Tissues: Evaluation of Octanol, Triolein, and Liposomes as Surrogates. *Environ. Sci. Technol.* **2014,** *48*, 5920-5928.

36. Chiou, C. T., Partition-coefficients of organic-compounds in lipid water-systems and correlations with fish bioconcentration factors. *Environ. Sci. Technol.* **1985,** *19*, 57-62.

37. Escher, B.; Abagyan, R.; M, E.; Klüver, N.; Redman, A.; Zarfl, C.; Parkerton, T., Recommendations for improving methods and models for aquatic hazard assessment of ionizable organic chemicals. *Environ. Toxicol. Chem.* **2020,** *39*, 269-286.

38. Henneberger, L.; Goss, K. U.; Endo, S., Partitioning of Organic Ions to Muscle Protein: Experimental Data, Modeling, and Implications for in Vivo Distribution of Organic Ions. *Environ. Sci. Technol.* **2016,** *50*, 7029-7036.

39. Henneberger, L.; Goss, K. U.; Endo, S., Equilibrium Sorption of Structurally Diverse Organic Ions to Bovine Serum Albumin. *Environ. Sci. Technol.* **2016,** *50*, 5119-5126.

40. Endo, S.; Bauerfeind, J.; Goss, K.-U., Partitioning of Neutral Organic Compounds to Structural Proteins. *Environ. Sci. Technol.* **2012,** *46*, 12697-12703.

41. Ulrich, N.; Endo, S.; Brown, T. N.; Watanabe, N.; Bronner, G.; Abraham, M. H.; Goss, K.-U., UFZ-LSER database v 3.2.1 [Internet], Leipzig, Germany, Helmholtz Centre for Environmental Research-UFZ. 2017 [accessed on 05.02.2021]. Available from http://www.ufz.de/lserd. **2021**.

42. Endo, S.; Escher, B. I.; Goss, K. U., Capacities of Membrane Lipids to Accumulate Neutral Organic Chemicals. *Environ. Sci. Technol.* **2011,** *45*, 5912-5921.

43. Endo, S.; Goss, K. U., Serum Albumin Binding of Structurally Diverse Neutral Organic Compounds: Data and Models. *Chem. Res. Toxicol.* **2011,** *45*, 2293-2301.

44. Smedes, F., Determination of total lipid using non-chlorinated solvents. *Analyst* **1999,** *124*, 1711-1718.

45. Niu, L.; Carmona, E.; Konig, M.; Krauss, M.; Muz, M.; Xu, C.; Zou, D.; Escher, B. I., Mixture Risk Drivers in Freshwater Sediments and Their Bioavailability Determined Using Passive Equilibrium Sampling. *Environ Sci Technol* **2020,** *54*, 13197-13206.

46. Neale, P. A.; Altenburger, R.; Ait-Aissa, S.; Brion, F.; Busch, W.; de Aragão Umbuzeiro, G.; Denison, M. S.; Du Pasquier, D.; Hilscherova, K.; Hollert, H.; Morales, D. A.; Novac, J.; Schlichting, R.; Seiler, T.-B.; Serra, H.; Shao, Y.; Tindall, A. J.; Tollefsen, K. E.; Williams, T. D.; Escher, B. I., Development of a bioanalytical test battery for water quality monitoring: Fingerprinting identified micropollutants and their contribution to effects in surface water. *Water Res.* **2017,** *123*, 734-750.

47. Escher, B. I.; Glauch, L.; Konig, M.; Mayer, P.; Schlichting, R., Baseline Toxicity and Volatility Cutoff in Reporter Gene Assays Used for High-Throughput Screening. *Chem. Res. Toxicol.* **2019,** *32*, 1646-1655.

48. Reiter, E. B.; Jahnke, A.; Konig, M.; Siebert, U.; Escher, B. I., Influence of Co-Dosed Lipids from Biota Extracts on the Availability of Chemicals in In Vitro Cell-Based Bioassays. *Environ. Sci. Technol.* **2020,** *54*, 4240-4247.

49. Anderson, J. M.; Ziats, N. P.; Azeez, A.; Brunstedt, M. R.; Stack, S.; Bonfield, T. L., Protein adsorption and macrophage activation on polydimethylsiloxane and silicone-rubber. *J. Biomat. Science-Polymer Edition* **1995,** *7*, 159-169.

50. Trudel, J.; Gauderer, M. W. L.; Drews, M. J.; LaBerge, M., Lipid uptake by silicone enteral access feeding devices. *J Pediatric Surgery* **1998,** *33*, 880-884.

51. Chumbimuni-Torres, K. Y.; Coronado, R. E.; Mfuh, A. M.; Castro-Guerrero, C.; Silva, M. F.; Negrete, G. R.; Bizios, R.; Garcia, C. D., Adsorption of proteins to thin-films of PDMS and its effect on the adhesion of human endothelial cells. *RSC Advanc.* **2011,** *1*, 706-714.

52. Zhang, K.; Pereira, A. S.; Martin, J. W., Estimates of Octanol-Water Partitioning for Thousands of Dissolved Organic Species in Oil Sands Process-Affected Water. *Environ. Sci. Technol.* **2015,** *49*, 8907-8913.

53. Reichenberg, F.; Smedes, F.; Jonsson, J. A.; Mayer, P., Determining the chemical activity of hydrophobic organic compounds in soil using polymer coated vials. *Chem. Cent. J.* **2008,** *2*, 8.

54. Jahnke, A.; McLachlan, M. S.; Mayer, P., Equilibrium sampling: Partitioning of organochlorine compounds from lipids into polydimethylsiloxane. *Chemosphere* **2008,** *73*, 1575-1581.

55. Allan, I. J.; Baek, K.; Haugen, T. O.; Hawley, K. L.; Hogfeldt, A. S.; Lillicrap, A. D., In Vivo Passive Sampling of Nonpolar Contaminants in Brown Trout (*Salmo trutta*). *Environ. Sci. Technol.* **2013,** *47*, 11660-11667.

56. Pei, Y. Y.; Li, H. Z.; You, J., Determining equilibrium partition coefficients between lipid/protein and polydimethylsiloxane for highly hydrophobic organic contaminants using preloaded disks. *Sci. Total Environ.* **2017,** *598*, 385-392.

57. Geisler, A.; Endo, S.; Goss, K.-U., Partitioning of Organic Chemicals to Storage Lipids: Elucidating the Dependence on Fatty Acid Composition and Temperature. *Environ. Sci. Technol.* **2012,** *46*, 9519-9524.

58. Smedes, F.; Rusina, T. P.; Beeltje, H.; Mayer, P., Partitioning of hydrophobic organic contaminants between polymer and lipids for two silicones and low density polyethylene. *Chemosphere* **2017,** *186*, 948-957.

59. US EPA, Chemistry Dashboard. **2020**, https://comptox.epa.gov/dashboard/ accessed on 20 Dec 2020.

60. Heltsley, R. M.; Cope, W. G.; Shea, D.; Bringolf, R. B.; Kwak, T. J.; Malindzak, E. G., Assessing Organic Contaminants in Fish: Comparison of a Nonlethal Tissue Sampling Technique to Mobile and Stationary Passive Sampling Devices. *Environ. Sci. Technol.* **2005,** *39*, 7601-7608.

61. Magnér, J. A.; Alsberg, T. E.; Broman, D., Evaluation of poly(ethylene-co-vinyl acetate-co-carbon monoxide) and polydimethylsiloxane for equilibrium sampling of polar organic contaminants in water. *Environ. Toxicol. Chem.* **2009,** *28*, 1874-1880.

62. Kwon, J. H.; Wuethrich, T.; Mayer, P.; Escher, B. I., Dynamic permeation method to determine partition coefficients of highly hydrophobic chemicals between poly(dimethylsiloxane) and water. *Anal. Chem.* **2007,** *79*, 6816-6822.

63. Endo, S.; Mewburn, B.; Escher, B. I., Liposome and protein-water partitioning of polybrominated diphenyl ethers (PBDEs). *Chemosphere* **2013,** *90*, 505-511.

64. Neale, P. A.; Antony, A.; Gernjak, W.; Leslie, G.; Escher, B. I., Natural versus wastewater derived dissolved organic carbon: Implications for the environmental fate of organic micropollutants. *Water Res.* **2011,** *45*, 4227-4237.

65. Smedes, F., SSP silicone-, lipid- and SPMD-water partition coefficients of seventy hydrophobic organic contaminants and evaluation of the water concentration calculator for SPMD. *Chemosphere* **2019,** *223*, 748-757.

66. Hsieh, M.; Fu, C.; Wu, S., Simultaneous Estimation of Glass–Water Distribution and PDMS–Water Partition Coefficients of Hydrophobic Organic Compounds Using Simple Batch Method. *Environ. Sci. Technol.* **2011,** *45*, 7785-7791.

67. Yates, K.; Davies, I.; Webster, L.; Pollard, P.; Lawton, L.; Moffat, C., Passive sampling: partition coefficients for a silicone rubber reference phase. *J. Environ. Monit.* **2007,** *9*, 1116-1121.

68. Pintado-Herrera, M. G.; Lara-Martín, P. A.; González-Mazo, E.; Allan, I. J., Determination of silicone rubber and low-density polyethylene diffusion and polymer/water partition coefficients for emerging contaminants. *Environ. Toxicol. Chem.* **2016,** *35*, 2162-2172.

69. Kramer, N. I.; van Eijkeren, J. C. H.; Hermens, J. L. M., Influence of albumin on sorption kinetics in solid-phase microextraction: consequences for chemical analyses and uptake processes. *Anal. Chem.* **2007,** *79*, 6941-6948.